



## Conformational Analysis of 9-Deoxo-9a-aza-9a- and 9-Deoxo-8a-aza-8a-homoerythromycin A 6,9-Cyclic Iminoethers

Gorjana Lazarevski\*, Mladen Vinković, Gabrijela Kobrehel and Slobodan Đokić

PLIVA - Pharmaceutical, Chemical, Food and Cosmetic Industry, Research Institute  
Prilaz baruna Filipovića 89, 41000 Zagreb, Croatia

Biserka Metelko

"Ruder Bošković" Institute, 41000 Zagreb, Croatia

**Abstract:** The conformation of 9a- **4** and 8a- **5** bicyclic iminoethers, the key synthetic intermediates of 15-membered AZALIDES was determined. The 2D NMR data and molecular modeling techniques were used to establish the predominant solution-state conformation. Conformational analysis suggests that in reduction of the iminoethers the smaller ring in both bicyclic compounds, as well as steric effects around the imidate group are reactivity-determined factors. The invariance in coupling constants indicates that **4** and **5** do not change conformation, when they go from a polar to a hydrophobic environment.

Azithromycin **1** is the first member of a new class of antibiotics called AZALIDES<sup>1,2</sup>. It differs structurally from erythromycin A **2** by insertion of a methyl-substituted nitrogen at 9a position in the lactone ring creating a 15-membered macrocycle. Recently, we have reported<sup>3</sup> the conformational analysis of **1** in solution based on NMR spectroscopy and molecular mechanics calculations (MMC).

The first step in the synthesis of **1** includes the conversion of 9(*E*)-hydroxyiminoerythromycin A **3a** to the 9-deoxo-9a-aza-9a-homoerythromycin A cyclic iminoether **4** by means of Beckmann rearrangement<sup>4</sup>. We have suggested that iminoether **4** arises by intramolecular interception of Beckmann rearrangement nitrilium intermediate with the C6 hydroxyl group. After J. C. Gasc et al.<sup>5</sup> had described the quantitative synthesis of 9(*Z*)-erythromycin A oxime **3b**, we prepared 8a-aza-8a-homoerythromycin A cyclic iminoether **5** by the analogous reaction sequence<sup>4</sup>. The structure **4** has the imino nitrogen atom exocyclic to a 5-membered ring containing the oxygen atom thereby giving rise to a 2-imino-tetrahydrofuran system. In contrast, in the second structure **5**, the imidate function (-N=C-O-) lies completely within a 6-membered ring creating a 5,6-dihydro-1,3-oxazine system.

The key reaction step in the synthesis of 15-membered azalides is the reduction of the imidate group in **4** and **5**. Compound **4** was readily reduced by catalytic hydrogenation (5% Pt/C, 20 x 10<sup>5</sup> Pa). However, the same reaction conditions failed to reduce compound **5**. Wilkening<sup>6</sup> confirmed our results, performing reduction of **5** under more vigorous conditions (PtO<sub>2</sub>, 140 x 10<sup>5</sup> Pa).

\*Unknown to us at the same time of our **3b** → **5** synthesis, compound **5** had been synthesized<sup>6</sup>



Table 1.  $^1\text{H}$  and  $^{13}\text{C}$  Chemical Shifts (ppm) and  $^1\text{H}$ - $^1\text{H}$  Coupling Constants (Hz) for 9a-4 and 8a-Iminoethers 5

Position	4				5				4	5
	$\text{CDCl}_3$		$[\text{2H}_6]\text{DMSO}$		$\text{CDCl}_3$		$[\text{2H}_6]\text{DMSO}$		$\text{CDCl}_3$	
	$\delta$ $^1\text{H}$	J(H,H)	$\delta$ $^1\text{H}$	J(H,H)	$\delta$ $^1\text{H}$	J(H,H)	$\delta$ $^1\text{H}$	J(H,H)	$\delta$ $^{13}\text{C}$	
1	-		-		-		-		178.1	177.7
2	2.73	2.4, 7.2	2.59	2.4, 7.2	2.76	2.5, 7.6	2.62	2.5, 7.3	44.3	44.0
3	3.93	2.3 (t)	3.71	2.4 (t)	4.02	2.4	3.81	2.4, (t)	76.3	76.6
4	1.88	6.9, 2.3, 7.6	1.73	m	1.99	7.3, 2.5	1.84	m	42.8	42.1
5	3.92	6.9	3.78	6.5	3.82	7.3	3.72	6.8	79.0	80.2
6	-		-		-		-		87.7	79.0
7a	2.02	8.6, 13.1	1.89	8.6, 12.7	1.90	5.6, 13.5	1.74	5.8, 12.9		
7b	1.57	10.6, 13.1	1.42	10.7, 12.7	1.26	ov	ov		36.9	32.1
8	2.79	8.6, 6.9, 10.6	2.73	8.6, m	3.44	5.6, 6.8	3.30	m	35.1	45.0
9	-		-		-		-		163.7	160.7
10	3.70	9.4, 6.4	3.45	9.3, 6.9	2.69	10.1, 7.0	2.41	10.3, 7.2	52.7	42.3
11	3.67	9.4	3.49	9.3	3.49	10.1	3.21	ov	72.0	70.1
12	-		-		-		-		75.1	75.8
13	4.94	10.4, 2.3	4.92	2.1, 10.4	4.91	10.5, 2.4	4.85	2.2, 10.4	77.6	77.4
14a	1.88	14.4, 7.3, 10.4	1.73	m	1.91	14.5, 7.4, 10.5	1.74	m		
14b	1.48	14.4, 7.3, 2.3	1.30	ov	1.47	14.5, 7.4, 2.4	1.35	ov	21.5	21.0
15	0.89	7.3	0.76	7.3	0.87	7.4	0.76	7.3	11.1	10.9
2Me	1.19	7.2	1.03	7.0	1.16	7.6	ov		13.1	16.5
4Me	1.12	7.6	0.99	7.4	1.09	7.5	0.97	7.6	9.2	8.5
6Me	1.43	s	1.30	s	1.40	s	1.26	s	25.8	23.9
8Me	1.21	6.9	1.07	6.8	1.16	6.8	ov		18.3	22.4
10Me	1.27	6.4	1.11	7.0	1.17	7.0	ov		16.3	17.1
12Me	1.10	s	0.93	s	1.15	s	ov		17.6	12.6
1'	4.49	7.4	4.42	7.6	4.49	7.3	4.41	7.4	102.6	102.5
2'	3.20	7.4, 10.4	3.07	7.6, 10.0	3.21	7.3, 10.2	3.07	7.8, 9.8	70.8	70.7
3'	2.37	10.4, 12.2, 3.5	2.48	10.5, m	2.45	10.2, 3.7	2.48	m	65.5	65.9
3'NMe <sub>2</sub>	2.29	s	2.24	s	2.29	s	2.20	s	40.3	40.3
4'a	1.69	12.8, 2.0, 3.5	1.61	10.5, m	1.70	12.2, 3.7	1.61	m		
4'b	1.23	12.8, 12.2,	1.02	ov	1.23	12.2, 10.0,	ov		28.6	28.6
5'	3.54	10.6, 6.3, 2.0	3.71	10.2, 1.9,	3.54	10.7, 5.9	3.72	m	68.7	68.9
5'Me	1.22	6.3	1.05	ov	1.23	5.9	ov		21.3	21.6
1''	5.19	4.6	4.87	4.5	5.04	4.7	4.70	4.3	94.5	94.7
2''a	2.44	15.3	2.34	14.7	2.44	15.3	2.33	15.2		
2''b	1.63	15.3, 4.6	1.49	4.8, 14.9	1.63	15.3, 4.7	1.50	4.4, 15.0	34.6	34.6
3''	-		-		-		-		73.0	73.1
3''Me	1.23	s	1.13	s	1.28	s	1.14	s		21.4
3''OMe	3.38	s	3.24	s	3.36	s	3.22	s	49.5	49.5
4''	3.08	9.5, 10.3	2.95	9.3	3.08	9.5	2.95	9.5	77.9	78.0
5''	4.11	9.5, 6.3	4.09	9.3, 6.3	4.11	9.5, 6.1	4.09	6.2, 9.3	65.8	65.7
5''Me	1.33	6.3	1.13	ov	1.33	6.1	1.14	ov	18.1	18.2

ov Overlapped.

*Conformational analysis*

The principal NMR determinants of the conformation of a molecule are coupling constants, which depend on dihedral angles, and nuclear Overhauser effect (NOE), which depend on proton-proton distances. An analysis of the  $^1\text{H}$  NMR coupling constants was used to compare the major solution-state conformation of **4** and **5**. A comparison of the  $^3J_{\text{H,H}}$  values in  $\text{CDCl}_3$  and the corresponding dihedral angles for vicinal proton pairs is given in Table 2. Analysis of the couplings using the modified Karplus equation<sup>10</sup> gave a series of

Table 2. Dihedral Angles Calculated from  $^1\text{H}$  -  $^1\text{H}$  Coupling Constants for 9a- **4** and 8a-Iminoethers **5**

Vicinal pair	<b>4</b>				<b>5</b>			
	$^3J_{\text{a}}^{\text{exp}}$ /Hz	$\Phi_{\text{calc}}^{\text{b}}$ /°	$\Phi_{\text{MM}}^{\text{c}}$ /°	$^3J_{\text{d}}^{\text{MM}}$ /Hz	$^3J_{\text{a}}^{\text{exp}}$ /Hz	$\Phi_{\text{calc}}^{\text{b}}$ /°	$\Phi_{\text{MM}}^{\text{c}}$ /°	$^3J_{\text{d}}^{\text{MM}}$ /Hz
Lactone								
H2 / H3	2.4	107	104	1.9	2.5	109	108	2.4
H3 / H4	2.3	- 54	- 66	1.1	2.4	- 54	- 68	1.0
H4 / H5	6.9	134	129	6.0	7.3	136	136	7.3
H7a / H8	8.6	- 26	- 29	8.2	5.6	- 41	- 46	4.8
H7b / H8	10.6	- 155	- 148	9.4	nd	nd	- 163	11.3
H10 / H11	9.4	160	169	9.9	10.1	153	168	11.4
H13 / H14a	2.3	59	70	1.3	2.4	62	66	1.6
H13 / H14b	10.4	-166	-171	11.7	10.5	-166	-174	11.7
Desosamine								
H1' / H2'	7.4	172	175	7.6	7.3	171	175	7.6
H2' / H3'	10.4	180	175	10.5	10.2	-176	178	10.5
H3' / H4'a	3.5	61	62	3.4	3.7	62	61	3.5
H3' / H4'b	12.2	180	179	11.8	12.2	180	179	11.8
H4'a / H5'	2.0	- 62	- 59	2.3	2.0	- 62	- 60	2.2
H4'b / H5'	10.6	168	176	11.3	10.7	169	177	11.4
Cladinose								
H1" / H2"a	nr		64	2.4	nr		65	2.3
H1" / H2"b	4.6	- 46	- 49	4.2	4.7	- 47	- 49	4.2
H4" / H5"	9.5	180	176	9.3	9.5	180	176	9.3

<sup>a</sup> Experimental values for **4** and **5** in  $\text{CDCl}_3$  at 293 K

<sup>b</sup> Dihedral angles  $\Phi_{\text{calc}}$  were calculated from  $^3J_{\text{exp}}$  using equation (1) by simple Turbo Pascal program

<sup>c</sup> Dihedral angles of solute state conformation predicted on base MMX calculation

<sup>d</sup> Coupling constants calculated for MMX solution state geometry using equation (1)

nd Not determined

nr Not resolved

Table 3. Qualitative NOE Data for 9a- 4 and 8a-Iminoethers 5

Position	4	5
Contact intraunits		
Aglycone ring		
2	4 (2.32), 2Me (2.53), 4Me (2.21)	4 (2.31), 2Me (2.60), 4Me (2.27)
3	4 (2.46), 11 (2.32)	4 (2.49), 5 (2.46), 11 (2.29)
4	5 (2.95), 4Me (2.49), 7a (2.20)	4Me (2.70), 7b (3.08)
5	6Me (2.70), 4 (2.95)	6Me (2.60)
7a	6Me (2.70), 7b (1.7)	7b (1.7)
8	6Me (2.57), 8Me (2.70)	6Me (2.65), 8Me (2.60)
10	10Me (2.60)	10Me (2.65)
11	12Me (3.00)	12Me (2.89)
13	15 (2.70)	
14a	14b (1.80), 15 (2.60)	15 (2.70), 14b (1.80)
14b	15 (2.60)	15 (2.70), 12Me (3.06)
6Me		10Me (3.15)
Desosamine		
1'	2' (3.10), 3' (2.50), 5' (2.40)	2' (3.10), 3' (2.53), 5' (2.38)
2'	3'NMe <sub>2</sub> (2.50), 4'a (2.58)	3'NMe <sub>2</sub> (2.50)
3'	4'b (2.49)	3'NMe <sub>2</sub> (2.60)
4'a	4'b (1.80)	4'b (1.80)
5'	5'Me (2.75)	5'Me (2.65)
3'NMe <sub>2</sub>		5'Me (2.70), 4'a (2.50)
Cladinose		
1''	2''a (2.52), 2''b (2.39)	2''a (2.52)
2''a	3''OMe (2.70), 2''b (1.77)	3''OMe (2.70), 3''Me (2.80), 2''b (1.8)
4''	3''Me (2.70), 5''Me (2.70)	3''Me (2.70), 5''Me (2.70)
5''	5''Me (2.60)	5''Me (2.70)
3''Me	3''OMe (2.60)	3''OMe (2.60)
Contact interunits		
Aglycone ring-sugar rings		
3	1'' (2.46)	1'' (2.48)
5	1' (2.31), 5'' (2.23)	1' (2.30), 5'' (2.13)
2Me	1'' (2.35)	1'' (2.80), 2''a (2.90), 3''OMe (3.11)
4Me	1' (2.46), 3''OMe (2.90)	1' (2.80), 3''OMe (2.85)
Desosamine-cladinose		
1'	3''OMe (2.63)	3''OMe (2.54)

Corresponding distances in Å between two protons (calculated solution-state) for 4 and 5 are in parentheses

dihedral angles. Because of the sinusoidal nature of the Karplus equation there are four solutions for a given coupling, but due to the bicyclic nature of these systems, only one is conformational reasonable or favored for any particular case. A summary of the observed NOE connectivities is shown in Table 3. NOESY Cross-peak analysis resulted in conformationally dependent distances which confirmed solution-state geometry of 4 and 5 obtained from calculated dihedral angles.

The observed vicinal coupling constants confirm that the cladinose and desosamine sugars adopt the same chair conformation found in the solution and X-ray structure of azithromycin<sup>3</sup>. The values for the three-bond H,H coupling constants of the lactone ring (Table 1) indicate that the region corresponding to these bonds (<sup>3</sup>J<sub>3,4</sub>, <sup>3</sup>J<sub>4,5</sub>, <sup>3</sup>J<sub>13,14a</sub>, <sup>3</sup>J<sub>13,14b</sub>) is in a similar conformation as that of 1. The small differences between theoretical and empirical values are attributed to a slight variation in the dihedral angles.

The small  ${}^3J_{2,3}$  value (2.3 Hz for **4** and 2.5 Hz for **5**) indicated that both compounds have "folded-in" C3-C5 fragment as was previously found in solution-state conformation of **1**. Rotation about C2-C3 and C5-C6 causes the C3-C5 part of the macrocyclic ring to "fold inwards" such that H3 gets closer to H11. The NOE between these two protons in **4** and **5**, which is an indication of "folded-in" conformation, was observed in all experiments (NOESY, NOE DIFF). Further, MMC confirmed NOE results giving calculated distances of 2.3 Å for both **4** and **5** in contrast to 3.1 Å for **1**. The smaller distance between H3 and H11 in compounds **4** and **5** is a result of the ring-contracted bicyclic system and is in agreement to that found for 14-membered macrolide antibiotic dirithromycin<sup>11</sup>. In addition,  ${}^3J_{2,3}$ , as well as the other coupling constants were invariant within experimental error when the spectra were obtained in solvents of differing polarity. This indicated a greater conformational rigidity for **4** and **5** and therefore a high conformational homogeneity in comparison with azithromycin. The relative large chemical differences between the diastereotopic protons at C7, C14, C2" and C4' also supported this conclusion<sup>12</sup>. However, the similarity in the  ${}^3J_{3,4}$  and  ${}^3J_{4,5}$  for all three compounds implies again that the orientation of the sugar rings with respect to one another and to the lactone ring is almost the same. NOE 4Me/3"OMe supported the proposed C3-C5 conformation which pushed the 4Me into a sterically congested environment.

Significant difference was observed for  ${}^3J_{10,11}$  which increases from 1.9 Hz in **1** to 9.4 and 10.1 Hz in **4** and **5**, resp. This was explained as a result of the 6,9 oxygen bridge since the similar value was earlier also found for bicyclic 6,9-erythromycin compounds<sup>13</sup>. Rotation around C10-C11 bond brought H10 and H11 protons in *anti* relationship (169°) in contrast to *gauche* relationship (74.6°) of these protons in **1**. Methyl on C10 is reoriented toward methyl on C6. Such spatial reorganization is justified by the presence of 10Me/6Me NOE in **5**. In compound **4** these methyls are in a similar orientation but spatially are more distant than in compound **5**. Molecular mechanics calculations were in agreement with the interpretation of the NMR data giving a distance of 3.4 and 3.1 Å for **4** and **5**, resp. It should be noted, however, that X-ray analysis of the 9a-iminoether aglycone<sup>4</sup> gave dihedral angle H11-C11-C10-H10 which corresponds closely with that found for **1**. Additional MM calculations showed that the X-ray conformation of the aglycone is in energy

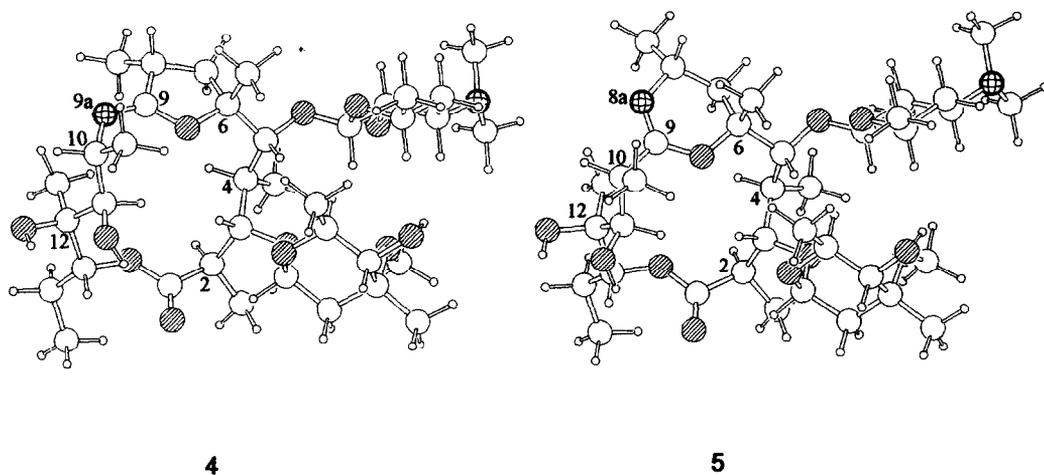


Figure 1. Ball-and-stick Representation of Solution-state Conformations of Iminoethers **4** and **5**.

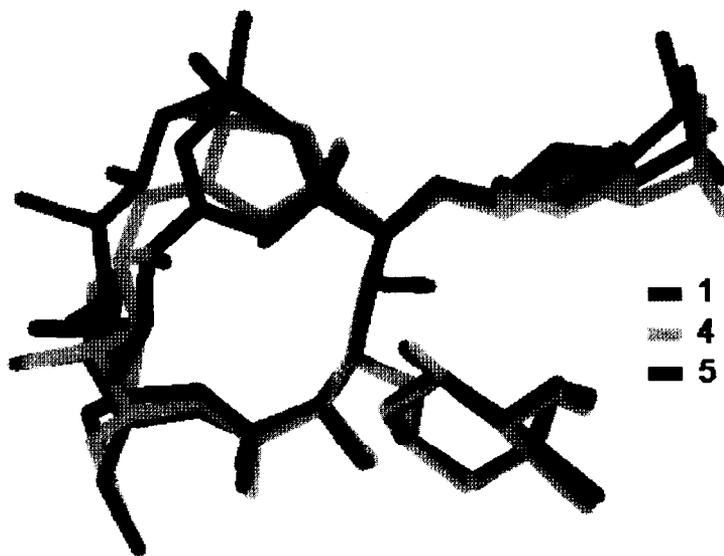


Fig. 2. Superposition of Solution-state Conformations of Compounds 1, 4 and 5.

3.09 kcal/mol lower than the solution-state conformation of 4. When sugar moieties were included, the solution-state conformation of 4 was the preferred one ( $\Delta E = 1.28$  kcal/mol).

Similar conformation of the larger ring in both bicyclic compounds indicated that it is not responsible for different reactivity. Thus it is reasonable to conclude that the smaller ring can be responsible for greater reactivity of 4 towards reduction. In the tetrahydrofuran ring of 4 four atoms C6-O6-C9-C8 are coplanar with C7 carbon under the others having an envelope-like conformation. The proof that C7 lies below the plane was provided by NOE H8/6Me (distance of 2.6 Å from the MMC). Dihedral angles calculated from  $^3J_{8,7a}$  and  $^3J_{8,7b}$  also are in agreement with the interpretation of the NMR data. Such arrangement ensures that the bulky C5 substituent occupies energetically favored equatorial position. These results are in excellent agreement with the X-ray data reported for 9a-iminoether aglycone ( $-33^\circ$  and  $-151^\circ$ , resp.).

In the compound 5, dihydro 1,3-oxazine ring adopts half-chair conformation. The two possible half-chair conformations that the oxazine ring can assume were taken into account. We found that C6 lies above the plane defined by C8-N8a-C9-O6, while C7 is situated at the same distance below the plane. This geometry ensures strain relief since the axial bonds at four atoms are converted to a less crowded pseudo axial position, while true axial and equatorial bonds are only that at C7 and C6. Such conformation also ensures that the bulky C10 and C5 substituents occupy pseudo equatorial and equatorial position, resp. In agreement with these conclusions were NOEs found for H8/6Me and 6Me/10Me and distances predicted from MMC.

NOE interactions and  $^1H$  NMR relaxation measurements ( $T_1$  data, Table 4) support the conformation depicted in Fig.1 and Fig. 2. The small  $^1HT_1$  value for 4Me is consistent with restricted mobility of this group in C3-C5 "folded-in" conformation. The relatively long  $^1HT_1$  values for 15Me, 5'Me and 3"OMe are indicative of near-free rotation. The remaining methyl groups have intermediate  $^1HT_1$  values.

Table 4. Experimental  $^1\text{H}$  NMR Relaxation Times ( $T_1$  in s,  $\text{CDCl}_3$ ) and Calculated Rotational Energy Barriers (Calculated Solution-state Conformation) for the Methyl Groups in **4** and **5**.

Methyl	<b>4</b>		<b>5</b>	
	$^1\text{H } T_1^a$	E <sup>b</sup>	$^1\text{H } T_1^a$	E <sup>b</sup>
15Me	0.54	A	0.56	A
3"OMe	0.49	A	0.47	A
5'Me	0.39	A	0.39	A
5"Me	0.38	A	0.38	A
8Me	0.38	B	0.31	B
3"Me	0.36	B	0.38	B
2Me	0.35	B	0.31	B
10Me	0.34	B	0.32	B
3'NMe <sub>2</sub>	0.32	B	0.35	B
6Me	0.30	B	0.37	B
4Me	0.25	C	0.29	C
12Me	0.24	C	0.27	C

<sup>a</sup> Experimental results at 300 MHz for **4** and **5** in  $\text{CDCl}_3$ ;  $T_1$ = spin-lattice relaxation time

<sup>b</sup> Theoretical calculations based on calculated solution-state conformations of **4** and **5**. The results are given in terms of energy ranges: A (2.0-3.5), B (3.5-5.0) and C (5.0-6.5)

### Conclusions

Conformational analysis suggests that a greater reactivity of 9a-iminoether **4** in comparison with its 8a-positional isomer **5** is a result of greater steric strains and therefore a higher energy in 5-membered ring of **4** than in the 6-membered ring of **5** (MM steric energies for corresponding 5-membered and 6-membered model ring systems, 8.41 and 2.81 kcal/mol, resp.). Further, steric effects about C=N double bond may be important in catalytic reduction<sup>14</sup>. Steric hindrance calculated as convex Connolly surface areas<sup>15</sup> (probe radii was 1 Å) for C9 in **4** was 0.093 Å<sup>2</sup>, while such area don't exists in **5**. This indicated easier approach of the **4** to the surface of catalyst.

After completing our studies we observed a report of Wilkening *et al.*<sup>16</sup>, who have found that for hydrogenation of **5** more vigorous conditions are required in comparison with 9,12 -cyclic-8a-iminoether which has the same 5-membered ring as compound **4**.

### Experimental

The  $^1\text{H}$  and  $^{13}\text{C}$  NMR spectra were acquired at ambient temperature in 5 mm o.d. NMR tubes on Varian Gemini 300 spectrometer. COSY spectra were acquired with sweep width of 3200 Hz into 1024 data points in F2 dimension. The 90° pulse was 15.0 μs, the relaxation delay was 1.0 s and each FID was acquired with 8 scans and 2 dummy scans. 256 Values of the evolution time were sampled but the data was zero filled to 1024 points in F1 prior to double Fourier transformation.

The HETCOR spectra were acquired with sweep widths of 8403.4 Hz into 2048 points in F2, and 4500.5 Hz into 256 points in F1 dimension, respectively. The 90° pulses for  $^1\text{H}$  and  $^{13}\text{C}$  were 15.3 and 13.0 μs, resp. Each FID was acquired with 256 scans and relaxation delay of 1.0 s. Experiments were acquired using standard Varian software.

The phase-sensitive NOESY experiment was performed using time-proportional-phase-increment method<sup>17</sup>. FID were acquired (64 scans, 2 dummy scans) over 3300.3 Hz into a 2K data block for 512

increment values of the evolution time,  $t_1$ . The raw data were zero filled to a 2K \* 2K matrix and processed with a 0.1 Hz line-broadening function in both dimensions. Experiments were performed with mixing time 0.45 s and the relaxation delay was 2.5 s.

The  $^1\text{H}$   $T_1$  experiment was conducted by using a standard inversion-recovery sequence ( $D_1$ -180°-VD-90°-FID) with relaxation delay 4 s and averaging 32 scans into an 16K data block (acquisition time 3.2 s). The experiment was repeated for 9 values of the variable delay VD ranging from 0.0156 to 4.0 s. The  $T_1$  values were calculated by using standard Varian software. The 180° pulse calibrated in  $\text{CDCl}_3$  solution was 15.0  $\mu\text{s}$ .

The  $^1\text{H}$  NOE difference spectra were acquired automatically using a modification of the method of Saunders<sup>18</sup>. Typically, 8-10 irradiations were performed in one experiment using 4 dummy scans and 32 scans at each frequency. The pulse sequence utilized a pre-irradiation delay (3 s), followed by a sub-saturating irradiation period (3-6 s), and then data acquisition with the decoupler gated off. Difference spectra were obtained by the subtraction of the control (off-resonance irradiation) from every other spectrum.

Calculations of dihedral angles from  $^3J_{\text{H,H}}$  values were performed using substituents electronegativity and orientation sensitive modified Karplus equation (1) by simple in house Turbo Pascal program based on graphic interpolation.

$$^3J_{\text{H,H}} = P_1 \cos^2\Phi + P_2 \cos\Phi + \sum \Delta\chi_i \{P_4 + P_5 \cos^2(\xi_j\Phi + P_6 |\Delta\chi_j|)\} \quad (1)$$

Empirical parameters  $P_1$ - $P_6$  used in equation (1) were there from original papers<sup>10</sup>,  $\chi$  was Huggins electronegativity of the substituents, and  $\xi$  was flag (+1 or -1) which represented orientation of the substituents.

Geometry of solution-state conformations of **4** and **5** were obtained by the following procedure. The azithromycin solution-state molecule was edited to the corresponding topology and  $^3J_{\text{H,H}}$  based dihedral angles using molecular graphics (Chem-X)<sup>19</sup>. Such structures were then optimised by Chem-X and finally by MMX<sup>20</sup> force field to geometry postulated as solution-state conformation.

Calculations of rotational barriers for methyl groups were performed by using MMX force field. Rotational energy barriers for each methyl were obtained through relaxation of molecule (energy minimization) at methyl-molecule dihedral angle rotated for 60 degrees from value of minimum energy conformation.

Connolly surfaces were calculated analytically by original in house Turbo Pascal program based on primal M. Connolly algorithm<sup>15</sup> with minor corrections and improvements.

### Acknowledgements

This work was supported in part by Grant-in-Aid from Ministry of Science, Technology and Informatics of Republic of Croatia (1-07-035). We also thank Mr. D. Vinković for work out the program for calculation of Connolly surface areas.

### References

- Đokić, S.; Kobrehel, G.; Lopotar, N.; Kamenar, B.; Nagl, A.; Mrvoš, D. *J. Chem. Res. (S)* **1988**, 152-153; (M) **1988**, 1239-1261.
- Bright, G. M.; Nagel, A. A.; Bordner, J.; Desai, K. A.; Dibrino, J. N.; Nowakowska, J.; Vincent, L.; Watrouws, R. M.; Sciavolino, F. C.; English, A. R.; Retsema, J. A.; Anderson, M. R.; Brennan, L. A.; Borovoy, R. J.; Cimochoowski, C. R.; Faiella, J. A.; Girard, A. E.; Girard, D.; Herbert, C.; Manousos, M.; Mason, R. *J. Antibiotics* **1988**, *41*, 1029-1047.
- Lazarevski, G.; Vinković, M.; Kobrehel, G.; Đokić, S.; Metelko, B.; Vikić-Topić, D. *Tetrahedron* **1993**, *49*, 721-730.

4. Đokić, S.; Kobrehel, G.; Lazarevski, G.; Lopotar, N.; Tamburašev, Z.; Kamenar, B.; Nagl, A.; Vicković, I. *J. Chem. Soc. Perkin Trans. 1*, **1986**, 1881-1890.
5. Gasc, J. C.; D'Ambriers, S. G.; Lutz, A.; Chantot, J. F. *J. Antibiotics* **1991**, *44*, 313-330.
6. Wilkening, R. R. *EPA 0 508 725 A1 (Merck)* **07. 04. 1992**.
7. Derome, A. E. *Modern NMR Techniques for Chemistry Research*; Ed.; Baldwin, J. E.; Pergamon Press; Oxford, 1985.
8. Breitmaier, E.; Voelter, W. *Carbon-13 NMR Spectroscopy*; Ebel, H. F. Ed; VCH Verlagsgesellschaft: Weinheim, 1987; pp. 213.
9. Eliel, E. L.; Bailey, W. F.; Kopp, L. D.; Willer, R. L.; Grant, D. M.; Betrand, R.; Christensen, K. A.; Dalling, D. K.; Duch, M. W.; Wenkert, E.; Schell, F. M.; Cochran, D. W. *J. Am. Chem. Soc.* **1975**, *97*, 322-330.
10. Haasnoot, C. A. G.; de Leeuw, F. A. A. M.; Altona, C. *Tetrahedron* **1980**, *36*, 2783-2792.
11. Everett, J. R.; Tyler, J. W. *J. Chem. Soc. Perkin Trans. 2* **1988**, 325-337.
12. Berg, J. E.; Laaksonen, A.; Wahlberg, I. *Tetrahedron* **1991**, *47*, 9915-9928.13.
13. Kibwage, I. O.; Busson, R.; Janssen, G.; Hoogmartens, J.; Vanderhaeghe, H.; Bracke, J. *J. Org. Chem.* **1987**, *52*, 990-996.
14. March, J. *Advanced Organic Chemistry; Reactions, Mechanisms and Structure*; Jonh Wiley and Sons, Inc.: New York, 1985; pp. 697.
15. Connolly, M. L. *J. Appl. Cryst.* **1983**, *16*, 548-558.
16. Wilkening, R. R.; Ratchliffe, R. W.; Doss, G. A.; Bartizal, K. F.; Graham, A. C.; Herbert, C. M. *Bioorganic & Medical Chem. Lett.* **1993**, *3*, 1287-1292.
17. Bodenhausen, G.; Kogler, H.; Ernst, R. R. *J. Magn. Reson.* **1984**, *58*, 370-388.
18. Saunders, J. K. M.; Mersh, J. D. *Prog. Nucl. Magn. Reson. Spectrosc.* **1982**, *15*, 353-400
19. Chem-X, Chemical Design Ltd., Oxon, England, **1993**
20. Gajewski, J. J.; Gilbert, E. K.; McKelvey, J. MMX. An Enhanced Version of MM2. In *Advances in Molecular Modeling*, 2, Liotta, D. Ed.; Jai Press, Greenwich, CT 1990.

(Received in UK 15 June 1994; revised 31 August 1994; accepted 2 September 1994)